
Biodiversity Change: A Spatiotemporal Machine Learning Approach to Detect Forest Canopy Height Changes across the U.S. West Coast

Anonymous Author(s)

Affiliation

Address

email

Abstract

1 Monitoring forest structural changes is critical for understanding biodiversity
2 dynamics and responding to natural disturbances such as wildfires. In this study,
3 we present a machine learning framework that combines optical remote sensing data
4 from HISTARFM Landsat product with spaceborne LiDAR measurements from the
5 GEDI mission to generate forest canopy height maps and detect structural changes
6 at 30-meter resolution across the U.S. West Coast. We developed ConvLSTM
7 models trained using monthly composites of Landsat data and annual GEDI-
8 derived RH98 canopy height metrics. Additionally, we explored two approaches
9 for incorporating uncertainty information into ML modeling process. Our best-
10 performing model achieved an RMSE of 7.536 and a Pearson's r of 0.847. Using
11 the trained model, we generated canopy height maps for 2019 and 2020 and
12 performed change detection by differencing these maps. Evaluation against 135
13 wildfire events yielded a moderate ROC AUC of 0.65. We analyzed detection errors
14 and outlined potential improvements from both data and modeling perspectives.

15 1 Introduction

16 Biodiversity encompasses the variety of life on Earth, including the diversity of forest structures,
17 species, and ecosystems. Forest structure, characterized by the spatial arrangement and physical
18 attributes of vegetation, plays a critical role in shaping biodiversity patterns. Structural metrics derived
19 from forest data are being recognized as effective proxies for biodiversity [11]. Remote sensing
20 technologies such as Light Detection and Ranging (LiDAR) and high-resolution satellite imagery
21 capture fine-scale structural variation over large spatial and temporal extents, enabling cost-effective
22 biodiversity assessment in areas where field inventories are impractical. Machine Learning (ML)
23 models, particularly Convolution Neural Network (CNN) and Long Short-Term Memory (LSTM), are
24 well-suited for analyzing the high-dimensional, unstructured remote sensing data [6, 14]. Together,
25 they have been effectively applied to geospatial tasks [9]. In this study, we explored spatiotemporal
26 ML techniques for detecting forest structural changes using remote sensing datasets from NASA
27 missions. Our key contributions include: (1) a novel use of Hierarchical Equal Area isoLatitude
28 Pixelation (HEALPix) for ML model validation, (2) a spatiotemporal ML model for generating
29 wall-to-wall canopy height maps, (3) incorporation of data uncertainty into model training, and (4) a
30 change detection analysis focused on wildfires.

31 2 Related Work

32 Traditional approaches for forest height estimation have relied heavily on airborne LiDAR, which
33 offers precise 3D structural information but is limited by high acquisition cost and low coverage [3, 7].

34 To address these limitations, scientists and engineers have explored the use of satellite-based data,
 35 including optical imagery, Synthetic Aperture Radar (SAR), and spaceborne LiDAR. When combined
 36 with traditional ML methods, they have been used to predict forest canopy height with reasonable
 37 accuracy. However, these methods often depend on manual feature engineering and may struggle
 38 to generalize across diverse forest types and conditions [13, 5]. Deep learning models have gained
 39 attention for their ability to automatically learn hierarchical spatial and temporal features from remote
 40 sensing data. These models have been successfully applied to forest canopy height estimation tasks
 41 using both optical and LiDAR-derived inputs [1, 14]. Recent efforts have introduced advanced
 42 architectures such as UNet [10] for semantic segmentation and LSTM-based networks for modeling
 43 long-range temporal dependencies. However, model generalizability remains a key challenge, particu-
 44 larly when transferring across regions with varying forest compositions and characteristics. This study
 45 builds on these foundations by developing a spatiotemporal Convolutional Long Short-Term Memory
 46 (ConvLSTM) model using an optical imagery dataset derived from NASA’s Landsat missions and
 47 LiDAR measurements from the GEDI mission to generate forest height maps and detect changes.

48 3 ML-Ready Data Sets

49 We focus on the Western US Pacific forests, as shown in the light-blue polygon in Figures 1 and 2, an
 50 ideal test region given their high biological and structural diversity, varied disturbance regimes, and
 51 dense coverage of training data availability. Our study targets RH98, the forest relative height at the
 52 98th percentile, retrieved at 30-meter resolution.

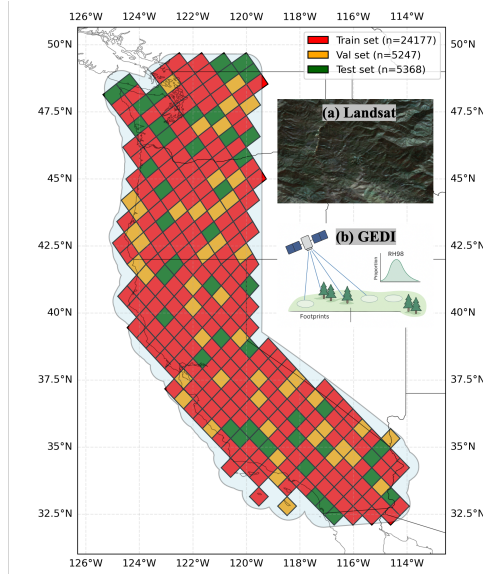


Figure 1: Train, validation, and test split

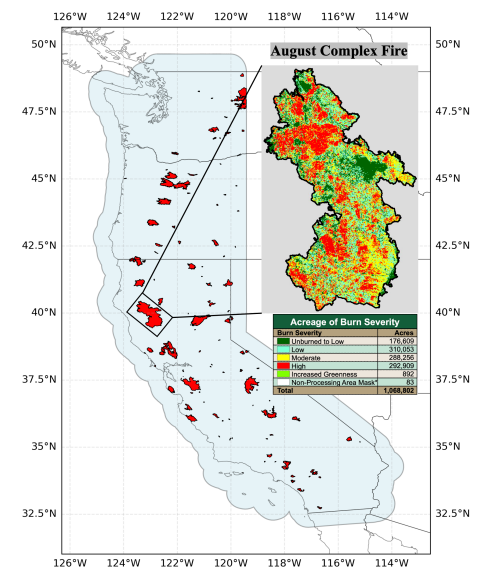


Figure 2: Wildfire events in 2020

53 **HISTARFM Landsat Optical Imagery:** The NASA Landsat program, operating since 1972,
 54 provides continuous multispectral imagery at 30-meter resolution, capturing visible, near infrared
 55 (NIR), and shortwave infrared (SWIR) bands via the Operational Land Imager (OLI) instrument. To
 56 minimize the impact of noise in raw Landsat data for ML models, we employ the Highly Scalable
 57 Temporal Adaptive Reflectance Fusion Model (HISTARFM) Landsat dataset [15], a gap-filled
 58 monthly reflectance time series generated by fusing Landsat and Moderate Resolution Imaging
 59 Spectroradiometer (MODIS) observations. An example visualized as an RGB image is shown in
 60 Figure 1 (a). For ML modeling, HISTARFM Landsat images are tiled into arrays of size 6 x 12 x
 61 224 x 224, where 6 corresponds to selected spectral bands (i.e., RGB, NIR, SWIR1, and SWIR2), 12
 62 corresponds to monthly observations, and 224 x 224 corresponds to spatial dimensions.

63 **GEDI LiDAR Measurements:** The Global Ecosystem Dynamics Investigation (GEDI) mission,
 64 launched aboard the International Space Station (ISS) in 2018, provides LiDAR waveforms at ~25
 65 meter footprints along orbital tracks between $\pm 51.6^\circ$ latitude [2]. Measurements are sampled every
 66 60 meters along the track, with 600 meters separating the individual laser beams, resulting in sparse

67 observations of vegetation structure and biomass. An artistic illustration is shown in Figure 1 (b). We
68 used the L2A Geolocated Elevation and Height Metrics product (via Google Earth Engine), filtered to
69 vegetation growing season (April to October) to limit the snow cover effect, restricted to full-power
70 beams with sensitivity greater than 0.9, and processed with respect to valid degradation and quality
71 flags. The data are resampled to 30-meter resolution, aligned with the HISTARFM Landsat reference
72 grid, and partitioned into 224 x 224 pixel tiles to use as the ground truth labels for ML models.

73 **Wildfire Dataset:** To evaluate change detection results, we compiled a wildfire dataset from the
74 Monitoring Trends in Burn Severity (MTBS) program. The dataset includes 135 wildfire events
75 from 2020 across California and the coastal regions of Oregon and Washington, each exceeding
76 1,000 acres. Locations of the wildfire events are shown in Figure 2. Burn severity classes (e.g., see
77 August Complex fire in Figure 2) for each event are provided as georeferenced raster files, which
78 were merged and resampled to the HISTARFM Landsat reference grid.

79 4 Methodology

80 **Spatial Validation:** We used a standard train, validation, and test split methodology to evaluate the
81 ML model. Because the tiles derived from the Landsat and GEDI data are spatially correlated, it
82 is critical to ensure spatial independence and prevent overlap across the splits. We present a novel
83 application of HEALPix to spatially divide the globe into equal-area regions for model validation [4].
84 The equal-area nature of the pixelization ensures that no regions are disproportionately represented.
85 The pixelization schema used for this study is shown in Figure 1. The dataset was partitioned into
86 70% for training, 15% for validation, and 15% for testing, corresponding to 24 177, 5247, and 5368
87 tiles, respectively.

88 **ML Training and Evaluation:** We employed a supervised regression framework to estimate forest
89 canopy height, using HISTARFM Landsat spatiotemporal tiles as input and GEDI-derived RH98
90 as ground truth. The backbone architecture was a ConvLSTM network, with the fully connected
91 layers in traditional LSTMs replaced by convolution operations to learn both spatial and temporal
92 patterns [12]. We explored three ConvLSTM variants: (1) a baseline model trained on the Landsat
93 spectral bands (i.e., RGB, NIR, SWIR); (2) a stacked model trained with six uncertainty bands
94 stacked onto spectral bands as input; and (3) a weighted-loss model in which the Mean Squared Error
95 (MSE) loss is weighed by the inverse of the corresponding uncertainty values. Hyperparameters
96 were tuned on the validation set via a small-scale grid search, with early-stopping applied to prevent
97 overfitting. Model performance was assessed using Root Mean Squared Error (RMSE) and Pearson
98 correlation coefficient on the train, validation, and test sets. Model bias was examined by computing
99 the best-fitting regression line between the predicted and ground truth GEDI RH98 values.

100 **Wall-to-wall Mapping and Change Detection:** After training and evaluation, the ML model was
101 applied to generate wall-to-wall prediction tiles across the study area. These tiles were georeferenced
102 and mosaicked to produce a forest canopy height map at 30-meter resolution. Change detection was
103 performed by aligning and differencing temporally distinct maps on a pixel-by-pixel basis. This
104 simple but effective approach captures the magnitude and direction of change, with positive and
105 negative values indicating gains and losses in forest canopy height.

106 5 Results and Analysis

107 **ML Results and Analysis:** The
108 test set results of the models are
109 summarized in Table 1. The
110 baseline model achieved the best
111 performance, with an RMSE of
112 7.536, Pearson’s r of 0.847, and
113 a regression slope of 0.80 (Fig-
114 ure 3). For the stacked model,
115 stacking uncertainty bands onto
116 the spectral bands negatively im-
117 pacted the model performance.
118 The performance degradation can be attributed to several factors. First, the inclusion of uncertainty

Table 1: Held-out test set results of the ML models.

Models	RMSE	Pearson’s r	Slope
Baseline model	7.536	0.847	0.80
Stacked model	9.195	0.780	0.64
Weighted-loss	7.868	0.830	0.77
Weighted-loss (threshold)	7.486	0.851	0.78

bands may have introduced noisy and low-signal information that did not contribute meaningfully to model training. Unlike the spectral bands that capture physical properties, uncertainty bands represent statistical variation, which may not carry spatial or temporal patterns that are directly relevant or predictive for GEDI RH98. Second, the model may have overfitted to uncertainty bands, causing it to prioritize uncertainty-related noise over the spatial and temporal patterns in the spectral bands. Third, the model architecture may not have been optimized to interpret uncertainty bands as a distinct type of input, thus failing to leverage its intended use. The weighted-loss model performed slightly worse than the baseline on the full test set, but outperformed the baseline when evaluation was restricted to low-uncertainty samples (i.e., 90.22% test set data included). This suggests that uncertainty-weighted training improves reliability on high-quality data, though predictions in high-uncertainty regions remain degraded. All three models exhibited bias towards under-predicting tall trees. This is likely due to the imbalanced nature of the GEDI data, with tall trees severely under-represented.

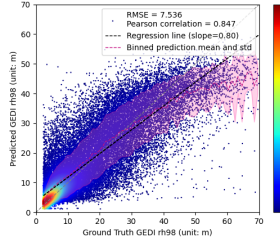


Figure 3: Test set performance for the baseline ML model

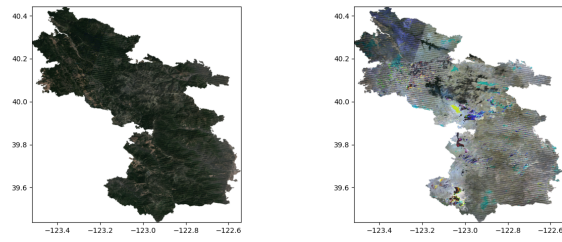


Figure 4: HISTARFM Landsat RGB images acquired in Aug. (left) and Sep. (right) 2020 for August Complex fire

131 **Change Detection Results and Analysis** To evaluate change detection, we generated wall-to-wall
 132 canopy height maps for 2019 and 2020 using the baseline ML model, and compared the differenced
 133 map with the 2020 wildfire events in Figure 2. The analysis focused on pixels labeled as the “High”
 134 and “Moderate” burn severity classes, as the “Unburned to Low” and “Low” burn classes generally
 135 do not correspond to measurable canopy height loss. The resulting Receiver Operating Characteristic
 136 (ROC) yielded an Area Under the Curve (AUC) of 0.65, which suggests that this approach has
 137 a moderate ability to distinguish between the “change” and “no change” classes. Still, often the
 138 two classes are not well-separated, leading to a moderate-to-high rate of false positive and false
 139 negative detections across various thresholds. These errors were caused by the ML model prediction
 140 imprecision, which likely stemmed from the model training being influenced by noisy data. For
 141 example, Figure 4 shows two HISTARFM Landsat images in August (left) and September (right) 2020
 142 for the California August Complex fire, which ignited on August 17, 2020. While the August image
 143 appears suitable for model training, the September image exhibits systematic horizontal striping
 144 artifacts across the entire image. With many other images with similar artifacts, the ConvLSTM
 145 model may overfit to the striping artifacts as false spatiotemporal signals, leading to reduced accuracy
 146 and generalizability. Moreover, the uncertainty bands failed to flag these artifacts as low-quality data,
 147 so even the weighted-loss model was unable to suppress their influence during model training.

148 6 Conclusion, Future Work, and Acknowledgment

149 In this paper, we presented a supervised ML method for detecting changes in forest canopy height
 150 using spatiotemporal HISTARFM Landsat and annual GEDI data at 30-meter resolution. While the
 151 method demonstrates moderate ability to distinguish between the “change” and “no change” classes,
 152 improvements are required to reduce false positives and false negatives before it can be deployed for
 153 real-world use cases. This is an ongoing effort, and we plan to address the identified problems from
 154 both data and modeling perspectives. To improve model robustness, we will incorporate Sentinel-1
 155 dual-polarization SAR data (i.e., HH and HV) from the European Space Agency (ESA), which may
 156 provide complementary information in regions where Landsat optical data are affected by noise or
 157 cloud contamination. To mitigate the systematic underestimation of tall trees, we will investigate
 158 post-hoc correction techniques and explore adapting Focal Loss [8] for regression tasks to better
 159 balance the influence of tall versus short trees during training. The acknowledgment statement here
 160 has been anonymized for double-blind review.

161 **References**

- 162 [1] Elias Ayrey and Daniel J. Hayes. The use of three-dimensional convolutional neural networks
163 to interpret lidar for forest inventory. *Remote sensing*, 10(4), 04 2018.
- 164 [2] Ralph Dubayah, James Bryan Blair, Scott Goetz, Lola Fatoyinbo, Matthew Hansen, Sean Healey,
165 Michelle Hofton, George Hurt, James Kellner, Scott Luthcke, John Armston, Hao Tang, Laura
166 Duncanson, Steven Hancock, Patrick Jantz, Suzanne Marselis, Paul L. Patterson, Wenlu Qi, and
167 Carlos Silva. The global ecosystem dynamics investigation: High-resolution laser ranging of
168 the earth's forests and topography. *Science of Remote Sensing*, 1, 06 2020.
- 169 [3] Ralph O. Dubayah and Jason B. Drake. Lidar remote sensing for forestry. *Journal of Forestry*,
170 98(6):44–46, 06 2000.
- 171 [4] Krzysztof M Gorski, Eric Hivon, Anthony J Banday, Benjamin D Wandelt, Frode K Hansen,
172 Mstvos Reinecke, and Matthia Bartelmann. Healpix: A framework for high-resolution dis-
173 cretization and fast analysis of data distributed on the sphere. *The Astrophysical Journal*, 622(2),
174 2005.
- 175 [5] Matthew C Hansen, Alexander Krylov, Alexandra Tyukavina, Peter V Potapov, Svetlana
176 Turubanova, Bryan Zutta, Suspense Ifo, Belinda Margono, Fred Stolle, and Rebecca Moore.
177 Humid tropical forest disturbance alerts using landsat data. *Environmental research letters*,
178 11(3), 03 2016.
- 179 [6] Sepp Hochreiter and Jurgen Schmidhuber. Long short-term memory. *Neural Computation*, 9(8),
180 1997.
- 181 [7] Michael A. Lefsky, Warren B. Cohen, Geoffrey G. Parker, and David J. Harding. Lidar
182 remote sensing for ecosystem studies: Lidar, an emerging remote sensing technology that
183 directly measures the three-dimensional distribution of plant canopies, can accurately estimate
184 vegetation structural attributes and should be of particular interest to forest, landscape, and
185 global ecologists. *BioScience*, 52(1):19–30, 01 2002.
- 186 [8] Tsung-Yi Lin, Priya Goyal, Ross Girshick, Kaiming He, and Piotr Dollar. Focal loss for dense
187 object detection. In *2017 IEEE International Conference on Computer Vision*, 2017.
- 188 [9] Markus Reichstein, Gustau Camps-Valls, Bjorn Stevens, Martin Jung, Joachim Denzler, Nuno
189 Carvalhais, and Prabhat. Deep learning and process understanding for data-driven earth system
190 science. *Nature*, 566, 02 2019.
- 191 [10] Olaf Ronneberger, Philipp Fischer, and Thomas Brox. U-net: Convolutional networks for
192 biomedical image segmentation. In *Medical Image Computing and Computer-Assisted Inter-
193 vention (MICCAI)*, pages 234–241. Springer, 2015.
- 194 [11] Fabian D Schneider, Felix Morsdorf, Bernhard Schmid, Owen L Petchey, Andreas Hueni,
195 David S Schimel, and Michael E Schaepman. Mapping functional diversity from remotely
196 sensed morphological and physiological forest traits. *Nat Commun*, 8(1), 11 2017.
- 197 [12] Xingjian Shi, Zhourong Chen, Hao Wang, Dit-Yan Yeung, Wai kin Wong, and Wang chun Woo.
198 Convolutional lstm network: A machine learning approach for precipitation nowcasting. In
199 *Advances in Neural Information Processing Systems*, volume 28, 2015.
- 200 [13] Marc Simard, Naiara Pinto, Joshua B. Fisher, and Alessandro Baccini. Mapping forest canopy
201 height globally with spaceborne lidar. *Journal of Geophysical Research: Biogeosciences*,
202 116(G4), 11 2011.
- 203 [14] Xiao Xiang Zhu, Devis Tuia, Lichao Mou, Gui-Song Xia, Liangpei Zhang, and Feng Xu. Deep
204 learning in remote sensing: A comprehensive review and list of resources. *IEEE Geoscience
205 and Remote Sensing*, 5(4), 12 2017.
- 206 [15] Álvaro Moreno-Martínez, Emma Izquierdo-Verdiguier, Marco P. Maneta, Gustau Camps-Valls,
207 Nathaniel Robinson, Jordi Muñoz-Marí, Fernando Sedano, Nicholas Clinton, and Steven W.
208 Running. Multispectral high resolution sensor fusion for smoothing and gap-filling in the cloud.
209 *Remote Sensing of Environment*, 247, 09 2020.